CrossMark

Performance investigation on fin type solar still with paraffin wax as energy storage media

T. R. Sathish Kumar[1] · S. Jegadheeswaran[2] · P. Chandramohan[1]

Abstract
It is indispensable to enhance the performance of a conventional solar still in order to increase its productivity. It has been effectively done by adding fins and thermal energy storage media to it. In the present work, the performance of a conventional single slope solar still is compared with an identical solar still with square pipes as fins attached to its basin liner. A thin layer of paraffin wax was stored beneath the basin liner as well as in the hollow space present in the square pipe fins as energy storage media. Experiments have been conducted on the conventional still for three different water depths, i.e. for 2, 3 and 4 cms. The masses for the corresponding water depths are 10 kg, 15 kg and 20 kg, respectively. The same water masses were maintained in the modified still, and experiments were conducted for the following cases: with mere fins and with fins cum energy storage media. The percentage increase in the efficiencies of the modified still with mere fins and with fins cum energy storage are observed as 64% and 95%, respectively.

List of symbols

q_g	Heat energy absorbed by the glass cover (W m^{-2})
I_s	Solar insolation on the glass cover (W m^{-2})
q_{lg}	Heat losses from the glass cover (W m^{-2})
q_{cg}	Heat losses from the glass cover to the surrounding air by convection (W m^{-2})
q_{rg}	Heat losses from the glass cover to the surrounding air by radiation (W m^{-2})
q_{lw}	Total heat losses of the basin water (W m^{-2})
q_{ew}	Evaporative heat losses of the basin water (W m^{-2})
q_{cw}	Convective heat losses of the basin water (W m^{-2})
q_{rw}	Radiation heat losses of the basin water (W m^{-2})
T_w	Temperature of basin water (K)
T_g	Temperature of glass cover (K)
Pw	Partial pressure of saturated water corresponding to basin water temperature (N m^{-2})
Pg	Partial pressure of saturated water corresponding to glass cover temperature (N m^{-2})

h_{cw}	Convective heat transfer coefficient between the saline water and the inner glass surface (W m^{-2} K^{-1})
h_{cg}	Convective heat transfer coefficient from the glass cover to the surrounding (W m^{-2} K^{-1})

Greek letters

α_g	Absorptivity of glass cover
τ_g	Transmissivity of glass cover
ε_w	Emissivity of the saline water surface
ε_g	Emissivity of the inner glass surface
σ	Stefan–Boltzmann constant

Subscripts, superscripts and acronyms

PCM	Phase change material
w	Basin water
g	Glass cover
c	Convection
r	Radiation

✉ T. R. Sathish Kumar
prof.trs@gmail.com

1 Department of Mechanical Engineering, Sri Ramakrishna Engineering College, Coimbatore, Tamil Nadu 641022, India

2 Department of Mechanical Engineering, Bannari Amman Institute of Technology, Sathyamangalam, Tamil Nadu 638401, India

Introduction

Water is the most essential substances on earth as all the living things must have water to survive. Today, the non-availability of fresh drinking water is a serious problem.

The freshwater resources are becoming scarce due to population growth and pollution caused by industrial waste. Drinking water shortage is expected to become one of the biggest problems faced by world. Contaminated water can transmit diseases such as diarrhoea, cholera, dysentery, typhoid and polio. By 2025, half of the world's population will be living in water-stressed areas [1]. The poor quality and quantity of drinking water have unfavourable effect on health and mortality of the children [2]. Several researchers have suggested a range of 2–5 L of fresh water per day for an individual to be adequate for survival [3].

In recent times, people have started to explore the availability of water resources in other planets too. As the name implies, thermal desalination process requires heat to convert the saline water into steam, and the steam or vapour is condensed to get fresh water. Fossil fuels can be used in the desalination process but this makes the system uneconomical [4]. An alternative source of energy for fossil fuel energy is the solar energy. Based on the growing emphasis on sustainability, solar energy proves to be one of the best eco-friendly source of energy for various applications like water pumping, space heating and energy storage [5–8]. In most cases, the direct use of sea water is not possible because it is made up of different types of salts. Distillation is a well-known process for the purification of saline water and most importantly water desalination process. One of the main advantages of the distillation process is that it requires heating only up to 120 °C, which can be supplied from solar energy or other cheap fuels. The distillation processes, such as multistage flash evaporation, reverse osmosis, electro dialysis, ion-exchange, phase change and solvent extraction, are energy intensive, expensive and uneconomical for small quantities of fresh water. On the other hand, the use of conventional energy sources, i.e. hydrocarbon fuels to drive these technologies has a negative impact on the environment. The desalination of available brackish or contaminated water in rural villages at a large scale is difficult due to the high cost associated with the construction and maintenance [9]. Kumar et al. [10] suggested that among the available desalination plants, a solar distillation plant with a capacity less than 200 kg day^{-1} is more economical. Solar energy is an abundant and safe source of vitality and therefore is distinguished as one of the most promising alternative energy choices because it is one of the readily available energy sources in the world.

A solar still is a product which uses the natural energy of the sun to convert impure water into potable water. The solar distillation by solar stills is particularly suitable for developing countries and especially in rural areas as it is more economic than other desalination technologies. A solar still works on two basic principles, namely evaporation and condensation. Initially the saline or brackish impure water that needs to be purified is poured into a basin with the black bottom. The solar still is then allowed to expose to the sun. The water gets heated utilizing the heat energy of the sun. After the water begins to evaporate, it begins to settle in the glass ceiling. The water gets condensed in the glass cover. Since the glass is inclined to a certain angle, the water droplets trickle down the glass and then it is collected separately. Solar still proves to be the best technical solution to supply fresh water to the remote villages without depending on high technology and expertise [11]. Plastic solar stills are preferred choice of solar still for commercial production amongst the various types of solar still tested till date [12].

Solar still integrated with fins in the flat plate basin decreases the preheating time required for evaporating the saline water. Fins increases the rate of heat transfer from the basin to the saline water thereby the productivity of the still is increased. Velmurugan et al. [13] conducted an experiment by integrating black rubber, sand, pebble or sponge immersed in brine in a fin type solar still. It is reported that the productivity has increased from 58 to 70%. Effective studies have been carried out after incorporating latent heat energy storage unit to the conventional system to enhance the efficiency of the system through energy storage [14–16].

Ramadan et al. [17] inferred in their work on fin type solar still that the daily productivity and efficiency increased due to the increase in the fin height and the same decreases with an increase in the fin thickness. Increasing the number of fins causes a decrease in the productivity of the fin type solar still due to the increased shadow area of the fins.

Rabhi et al. [18] performed an experiment in a solar still integrated with simple pin fins, and the results show that the distilled water production increased by 14.53% compared to the conventional solar still. Namprakai et al. [19] performed an experiment to evaluate the thermal performance of an ethanol solar still with fin plate to increase productivity. They concluded that the integration of fin into the basin solar still could increase productivity. Moreover, adding fin to the basin decreases the preheating time required for evaporation in the still basin, due to the increased effective absorption of basin plate and the solution temperature.

Omar et al. [20] conducted experimental studies on vertical finned passive solar stills and corrugated stills. It is observed that there is an increase in productivity of 40% and 21% for vertical finned and corrugated stills when compared to the conventional still. El Sebaii et al. [21] optimized the number of fins in the still and conducted investigations to find 13.7% improvement in the productivity. Alaian et al. [22] performed an experimental

investigation on the performance of solar still augmented with pin-finned wick. It is reported that there is an enhancement on the still productivity, efficiency and hence an enhancement of 23% system productivity when pin-finned wick is applied. Rajaseenivasan et al. [23] conducted experimental investigations on stills with circular and square fins and compared the performance results with the results of the same stills when the fins are covered by wick material and observed considerable increase in productivity in second case when compared to the first case. Velmurugan et al. [24] conducted performance studies on passive still with vertical fins. The results showed 45.5% increase in productivity when compared to conventional still.

Agarwal et al. [25] proposed a basin type solar still with porous fins made up of blackened old cotton rags partially dipped in the basin water, while the rest of the part extended above the basin water surface. It is established that the distillate production increases with the decrease in the basin water depth and the experimental results are in fair agreement with that obtained by the thermal model. El Sebaii et al. [26] conducted a year-round performance studies on finned solar still and inferred that the increased productivity of the finned still in summer is slightly higher than the increased productivity during winter. Though lot of research works have been carried out in solar still incorporated with different fin configurations, there arouse a need to investigate the performance of finned solar still integrated with thermal energy storage which has not been tried till date. To fulfil this need, in the present work a modified solar still with square pipes as fins is attached to the basin liner where the hollow space in the square pipe is filled with energy storage material. Here, paraffin wax is used as phase change material for storing excess energy during peak sunshine hours and to deliver the stored energy during off-sunshine hours to further enhance the productivity of the still.

The objective of the present work is to;

(1) To compare the performance of the conventional single slope solar still and solar still integrated with square pipes without thermal energy storage unit.

(2) To compare the performance of the conventional single slope solar still and solar still integrated with square pipes along with thermal energy storage unit filled with paraffin wax.

Materials and methods

Experimental set-up

Figures 1 and 2 show the schematic diagram and the photograph of the present single slope solar still which consists of a shallow rectangular basin made up of galvanized iron sheet of area 0.5 m^2 and thickness 1.006 mm. The absorber plate was painted with low reflectivity black paint, achieving matte finish to capture maximum solar incident radiation. A transparent tempered glass of 4 mm thickness was used to cover the top of the basin. A thin layer of paraffin wax was used as thermal energy storage material, beneath the basin liner as well as in the hollow square fins. The properties of the paraffin wax are furnished in Table 1. The glass tilt angle of the glazing was fixed as 12° which is close to the latitude of the experimental location Coimbatore, South India, 11°1N to trap maximum solar radiation into the solar still. The inclined face of the still was placed facing south since the test location was in northern hemisphere. K-type (Chromel–Alumel) thermocouples were placed appropriately to measure temperatures of basin water, glazing temperature, still chamber temperature and ambient temperature. A 12 point temperature indicator was used to receive signals from the thermocouples and indicate the values of temperature from various cardinal points in the experimental set-up. The entire still was housed inside a wooden casing of wall thickness 2 cm which also performed as insulator. A solarimeter was used to measure the global solar radiation falling on the collector area.

Experimental procedure

The brackish water was stored in the still in such a way that the basin is partially filled through inlet port. Major portion of the incident solar radiation was transmitted through the transparent glass cover leaving behind the lost radiations through reflection and absorption by glass cover. The transmitted radiation was again absorbed and reflected by the basin water mass. At the end, incident radiation reached the matte black surface present in the basin plate. The basin linen absorbed most of the incident solar radiation and passed most of the thermal energy generated to the water mass present in the basin. Major amount of heat loss from the basin water to the atmosphere was curtailed by placing the basin in a wooden casing which performed as a supporting structure as well as insulating chamber [24]. As the intensity of incident solar radiation progressed during the day, the basin water got heated up giving rise to difference in basin water and glass cover temperatures. The evaporative heat transfer between the water surface and glass inner surface increased with increase in the difference between their temperatures. The evaporated vapour got condensed upon cooling below the saturation temperature when it touched the glass inner surface. The condensed water dribbled down the inner surface of the inclined glazing and dropped on the collecting channel which is connected to the storage bottle through outlet port of the

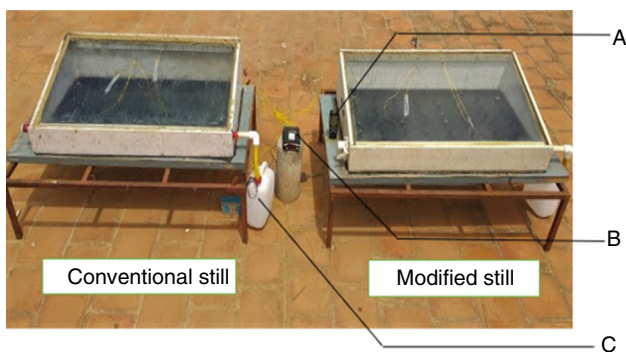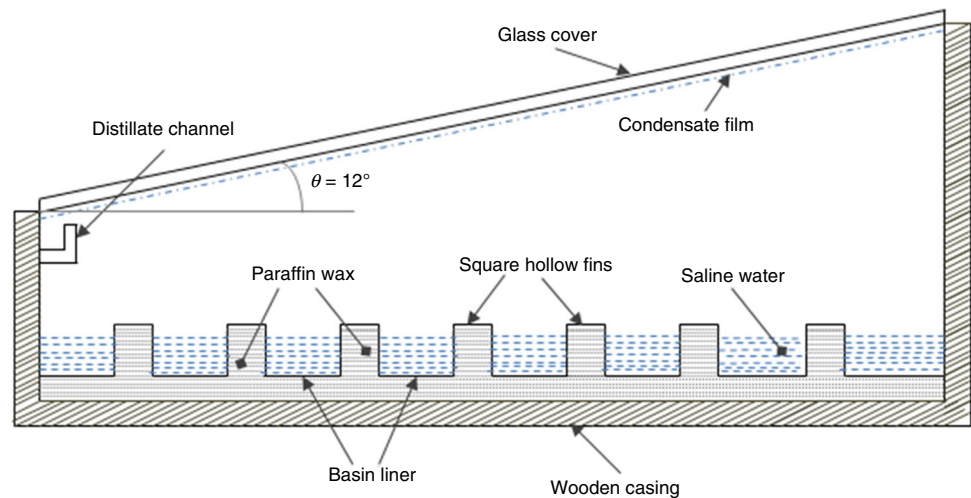**Fig. 1** Schematic view of the finned solar still with energy storage

Fig. 2 Photograph of the experimental set-up. **a** Solarimeter. **b** Temperature indicator. **c** Distillate collecting jar

still. The heat energy received by the glass cover from the water vapour is lost to the surrounding atmosphere by radiation and convection.

The finned solar still was coupled with an energy storage unit placed beneath the absorber basin where varied quantities of paraffin wax (2 kg, 3 kg and 5 kg) were placed to store excess energy received during the peak sunshine hours and deliver the same to the saline water in the basin during the off-sunshine hours, thereby extending the productivity of the still. The daily yield was higher for the solar still with 3 kg of paraffin wax compared to the rest. Hence, 3 kg of paraffin wax was chosen to be used as optimum energy storage material for solar still.

Energy analysis of the solar still

The following conditions were assumed and the energy balance for each of the components present in the solar still was arrived;

(1) Temperature stratification along the water column and glass thickness as nil.
(2) The entire system is vacuum tight and there is no air leakage from the corners of the glass cover.

Figure 3 shows the energy balance diagram for the four important components of the experimental set-up, i.e. glass cover, basin water, basin liner and PCM.

Energy balance for glass cover

The heat energy absorbed by the glass cover is given as [4],

$$q_g(W\ m^{-2}) = \propto_g I_s - q_{lg} \qquad (1)$$

where I_s is the solar insolation on the glass cover, q_{lg} is the heat losses from the glass cover to the surrounding air by convection and by radiation ($q_{cg} + q_{rg}$) [4]

$$q_{cg}(W\ m^{-2}) = h_{cg}(T_g - T_o) \qquad (2)$$

where h_{cg} is the heat transfer coefficient from the glass cover to the surrounding which is a function of wind speed (W_s) and can be calculated using the following relation [4]

Table 1 Properties of the PCM [21]

Property	Density, solid/liquid/kg m^{-3}	Specific heat, solid/liquid/J kg^{-1} K^{-1}	Thermal conductivity/W m^{-1} K^{-1}	Melting point/°C	Latent heat of melting/kJ kg^{-1}
Paraffin wax	818/760	2950/2510	0.24	56	226
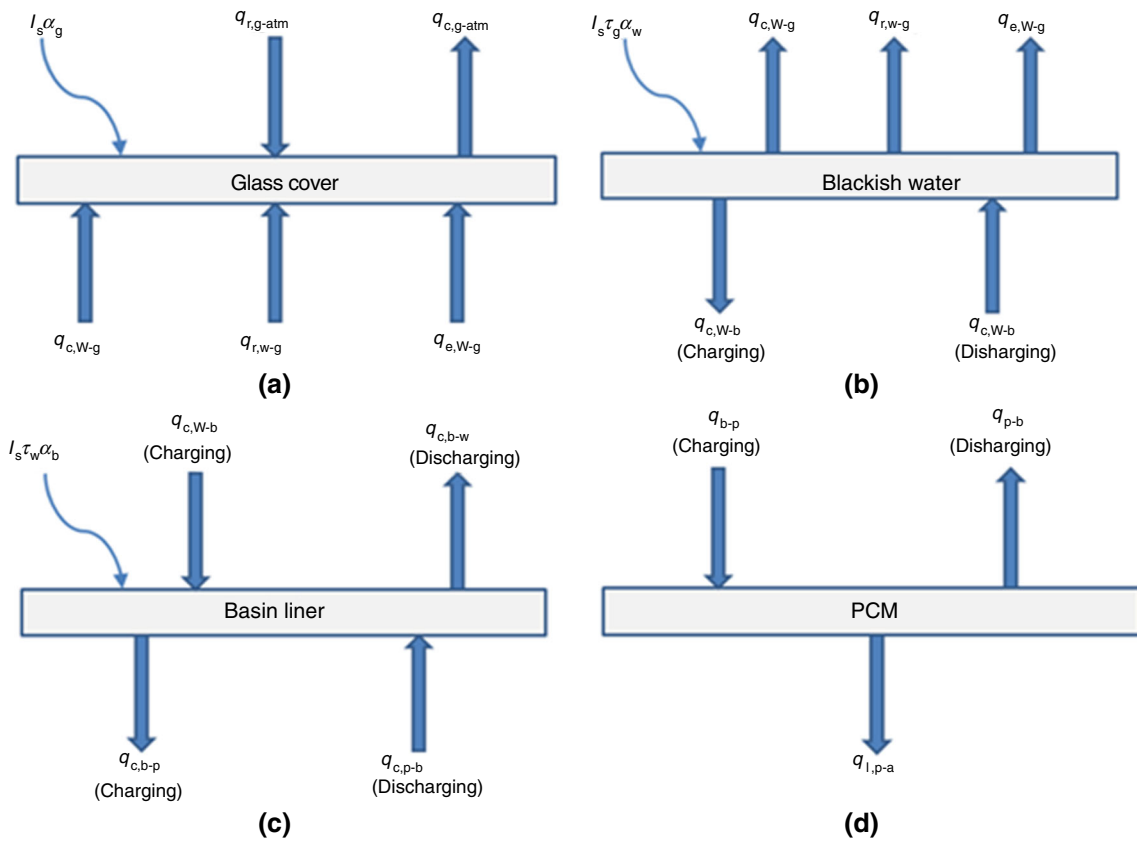
Fig. 3 Energy balance diagram of **a** glass cover, **b** brackish water, **c** basin liner and **d** PCM

$$h_{cg}\left(W\ m^{-2}\ K^{-1}\right) = 5.7 + 3.8W_s \quad (3)$$

$$q_{cg}\left(W\ m^{-2}\right) = \varepsilon_g \sigma\left[T_g^4 - (T_a - 11)^4\right] \quad (4)$$

where ε_g is the emissivity of the inner glass surface = 0.89, σ is Stefan–Boltzmann constant = 5.669×10^{-8} W m^{-2} K^{-4}

Energy balance for basin water

The heat absorbed by the water stored in the basin of area 1 m^2 is given as [4],

$$q_w\left(W\ m^{-2}\right) = \tau_w \propto_w I_s - q_{lw} \quad (5)$$

where q_{lw} is the total heat losses of the basin water which is given as [4],

$$q_{lw}\left(W\ m^{-2}\right) = q_{ew} + q_{rw} + q_{cw} + q_{lb} \quad (6)$$

where q_{ew} is the evaporative heat transfer rate at the saline water surface and is the function of yield of the still (W_p, L m^{-2} h^{-1}), given as,

$$q_{ew}\left(W\ m^{-2}\right) = \frac{\left(W_p \times 10^{-6} \times \rho_w L_w\right)}{3600} \quad (7)$$

where L_w is the latent heat of water which is equal to 2.4×10^6 J kg^{-1} [4].

$$q_{rw}\left(W\ m^{-2}\right) = F_{(w-g)}\sigma\left(\varepsilon_w T_w^4 - \varepsilon_g T_g^4\right) \quad (8)$$

where $F_{(w-g)}$ is shape or view factor which depends upon the geometry of the still. The value of shape factor is taken as 0.9 by approximating the geometry by two parallel planes. ε_w is the emissivity of saline water surface and ε_g is the emissivity of the inner glass surface whose values are 0.96 and 0.85, respectively.where q_{cw} is the convective heat transfer rate between the saline water and the inner glass cover surface which is given as [4],

$$q_{cw}\left(W\ m^{-2}\right) = h_{cw}\left(T_w - T_g\right) \quad (9)$$

where h_{cw} is the convective heat transfer coefficient between the saline water and the inner glass surface of the still which can be calculated using the relation [4],

$$h_{cw}(\text{W m}^{-2}) = 8.84 \times 10^{-4} \left[\frac{(P_w - P_g)T_w}{2.69P_a - P_w} + (T_w - T_g) \right]^{\frac{1}{3}} \tag{10}$$

where P_w, P_{wg} and P_a are vapour pressures of water at water surface temperature, glass cover temperature and at atmospheric pressure respectively, N m^{-2}. where q_{lb} is the heat losses by convection through the base of the basin and side walls to the surrounding which is given as [4],

$$q_{lb}(\text{W m}^{-2}) = h_{lb}(T_w - T_a) \tag{11}$$

where h_{lb} is the equivalent heat transfer coefficient by convection from the basin to the surrounding and is derived from the following equation [4],

$$h_{lb}(\text{W m}^{-2}\,\text{K}^{-1}) = \frac{k_{ins}}{X_{ins}} \tag{12}$$

where k_{ins} and the x_{ins} are values of thermal conductivity and the thickness of the insulation material.

Energy balance for the thermal energy storage layer

Thermal energy storage material feed the solar still during the absence of effective solar insolation over the system. The aim of using the thermal energy storage layer is to increase the distillate water output per day. The governing equation during daytime is given as [16],

$$q_{pd}(\text{W m}^{-2}) = m_p c_p \frac{\partial T_{pd}}{\partial t} \tag{13}$$

$$q_{pd}(\text{W m}^{-2}) = A_p I_s(\propto \tau)_p + A_w I_s(\propto \tau)_w - q_{lp} \tag{14}$$

During night time the equation is given as [16],

$$q_{pn}(\text{W m}^{-2}) = m_p c_p \frac{\partial T_{pn}}{\partial t} \tag{15}$$

$$q_{pn}(\text{W m}^{-2}) = m_p c_p \frac{\partial T_{pd}}{\partial t} + m_w c_{pw} \frac{\partial T_w}{\partial t} - q_{lp} \tag{16}$$

where m_p and m_w are the mass of thermal energy storage material and the saline water respectively in kg, A_p and A_w are the surface area of the thermal energy storage material and the saline water in m^2, $(\alpha\tau)_p$ and $(\alpha\tau)_w$ are the absorptivity and transmissivity of the thermal energy storage layer and the saline water respectively, q_{lp} is the heat losses between the thermal energy storage layer and the saline water in W m^{-2}.

The efficiency of the solar still integrated with thermal energy storage is evaluated by the ratio of daily yield (W_p, L m^{-2} day^{-1}) of the still to the total solar energy (q_t, W m^{-2}) utilized for the evaporation of the water in the basin of the basin. The equations to determine the efficiency of the still are as follows [16],

$$q_t(\text{W m}^{-2}) = q_g + q_w + q_p \tag{17}$$

$$W_p(\text{L m}^{-2}\,\text{day}^{-1}) = \frac{q_{ew}}{\rho_w L_w} \tag{18}$$

$$\eta_p = \frac{q_{ew}}{q_t} = \frac{h_{ew}(T_w - T_g)}{I_t} = \frac{2.35\rho_w \times W_p}{3600 I_s} \tag{19}$$

where I_s is the daily total solar radiation, J m^{-2} day^{-1}, W_p is the daily yield of the still, L m^{-2} day^{-1}, and L_w is the latent heat of the water evaporated which is equal to 2.35×10^6 J kg^{-1}.

The instantaneous efficiency of the still is determined using the following equation,

$$\eta_i = \frac{q_{ew}}{I_t} = \frac{h_{ew}(T_w - T_g)}{I_t} \tag{20}$$

$$h_{ew}(\text{W m}^{-2}) = 16.273 \times 10^{-3} \times h_{cw} \left[\frac{P_w - P_g}{T_w - T_g} \right] \tag{21}$$

where I_t is the hourly solar radiation, W m^{-2}, h_{ew} is the evaporative heat transfer coefficient, W m^{-2} K^{-1}, P_w and P_g are the partial saturation pressures for the corresponding water and glass temperatures, N m^{-2}. Figure 4 shows the thermal resistance network between the basin water and the PCM.

Exergy analysis of the solar still

Exergy is defined as the maximum amount of work that can be achieved by a system or flow of energy or mass when it comes to equilibrium condition with the reference surrounding. The first law analysis deals with the conservation
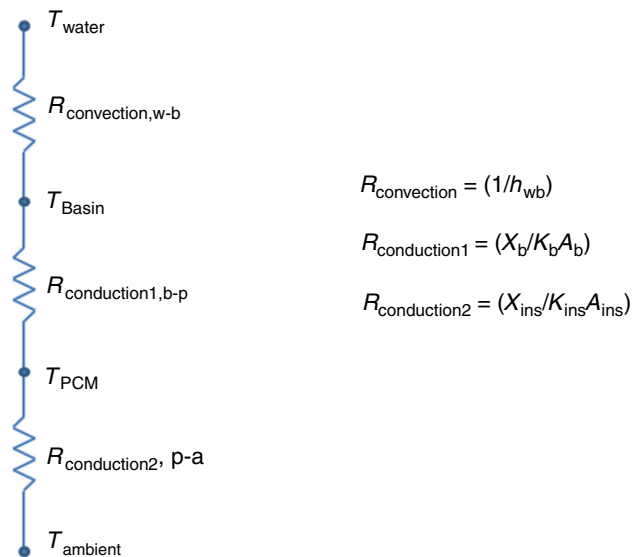

$R_{convection} = (1/h_{wb})$

$R_{conduction1} = (X_b/K_b A_b)$

$R_{conduction2} = (X_{ins}/K_{ins} A_{ins})$

Fig. 4 Schematic representation of thermal resistance network between basin water and PCM

of energy and hardly states information on degradation of system performance and its effect on output. The second law analysis or exergy analysis is found to be a useful tool to evaluate the performance of any energy system [27]. The exergy efficiency of the solar still is defined as the ratio of exergy output associated with the distillate water collected to the exergy input, which is through incident solar radiation. The exergy efficiency can also be expressed as a measure of unavailability due to exergy destruction [28].

$$\eta_{EX} = \frac{Ex_{output}}{Ex_{input}} = \frac{Ex_{evop}}{Ex_{sun}} = 1 - \frac{Ex_d}{Ex_{sun}} \qquad (20)$$

The hourly exergy of the solar still can be determined using the following expression [28],

$$Ex_{output} = Ex_{evap} = \frac{\dot{m}_{ew} \times L}{3600}\left(1 - \frac{T_a + 273}{T_w + 273}\right) \qquad (21)$$

where m_{ew} is the hourly yield of the solar still (kg h^{-1}), L is the latent of vapourization (J kg^{-1}), T_a and T_w are surrounding temperature and the basin water temperature (°C).

The exergy input can be determined using the following expression [28],

$$Ex_{input} = Ex_{sun} = A_s \times I(t)\left[1 - \frac{4}{3}\left(\frac{T_a}{T_s}\right) + \frac{1}{3}\left(\frac{T_a}{T_s}\right)^4\right] \qquad (22)$$

where Ex_{sun} is the exergy input to solar still through solar insolation, A_s is the area of the basin liner (m^2), $I(t)$ is the intensity of solar radiation (W m^{-2}) and T_s is the temperature of sun (6000 K).

The following expressions present the exergy flow analysis and its destruction in various components of a single slope passive solar still.

Glass cover

Out of total solar radiation falling over the surface of the glass cover, the glass absorbs a part of incident radiation ($\alpha_g Ex_{sun}$). The exergy balance for glass cover is given as [28],

$$Ex_{d,g} = \alpha_g Ex_{sun} + Ex_{t,w-g} - Ex_{t,g-a} \qquad (23)$$

where $Ex_{d,g}$ is the exergy destroyed in the glass cover, α_g is the absorptivity of the glass, $Ex_{t,w-g}$ is the exergy corresponding to heat transfer between basin water and glass inner surface, $Ex_{t,g-a}$ is the exergy corresponding to heat transfer between glass outer surface and the ambient air [28],

$$Ex_{t,w-g} = Ex_{evap} + Ex_{conv-w-g} + Ex_{rad-w-g} \qquad (24)$$

$$Ex_{t,g-a} = Ex_{rad-g-a} + Ex_{conv-g-a} \qquad (25)$$

where Ex_{evap} is the exergy of evaporation, $Ex_{conv-w-g}$ is the exergy due to convection between basin water and glass inner surface, $Ex_{rad-w-g}$ is the exergy due to radiation between basin water and glass inner surface, $Ex_{rad-g-a}$ is the exergy due to radiation between glass outer surface and ambient air, $Ex_{conv-g-a}$ is the exergy due to radiation between glass outer surface and ambient air.

Basin water (saline water)

The exergy destruction in the basin water is given by [28],

$$Ex_{d,w} = \tau_g \alpha_w Ex_{sun} + Ex_{b-w} + Ex_{t,w-g} \qquad (26)$$

where ($\tau_g \alpha_w Ex_{sun}$) is the incident solar energy absorbed by the basin water, Ex_{b-w} is the exergy due to heat transfer between basin liner and water, and

$$Ex_{b-w} = h_{conv-b-w}(T_b - T_w)\left(1 - \frac{T_a}{T_b}\right) \qquad (27)$$

where $h_{conv-b-w}$ is the convective heat transfer coefficient between the basin liner and the water.

Basin liner (including attached fins)

The exergy balance in basin liner is expressed by the equation [28],

$$Ex_{d,b-ch} = (\tau_g \tau_w \alpha_b)Ex_{sun} - (Ex_{b-w} + Ex_{b-pcm-ch}) \qquad (28)$$

where ($\tau_g \tau_w \alpha_b Ex_{sun}$) is the net solar exergy quantity absorbed by the basin liner, (Ex_{b-w}) is the exergy received by basin water, ($Ex_{b-pcm-ch}$) is the exergy share to phase change material and ($Ex_{d,b-ch}$) is the destroyed exergy.
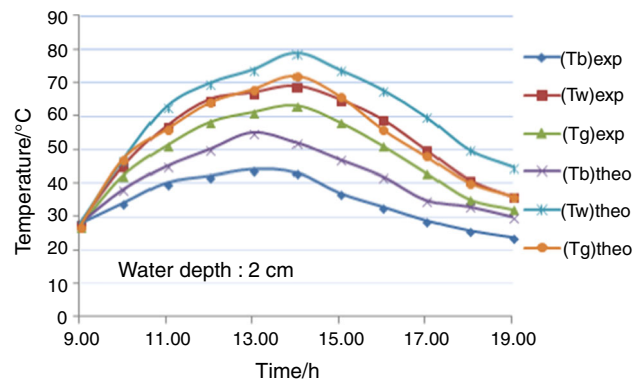

Fig. 5 Hourly variations of theoretical and experimental values of glass cover temperature, basin water temperature and basin liner temperature

Results and discussion

Figure 5 illustrates the hourly variations of the theoretical and the experimental values of glass temperature, basin water temperature and basin liner temperature. It is evident that the theoretical and the experimental values of temperatures of glass cover, basin water and basin liner are in good agreement.

Effect of water depth on productivity

Figure 6 summarizes the hourly variations of productivity with time period of the day for solar still with different basin water depths. The plot shows that though the productivity is more for solar still with 2 cm water depth during forenoon session, it drastically reduces during the post noon session compared to the results obtained through the other two basin water depths. The case is vice versa for 4 cm water depth. The productivity of solar still at 3 cm basin water depth is found to be in between the previous two cases. From the above observations, it is obvious that the incorporation of fins and energy storage to the conventional still with 2 cm basin water depth will yield highest productivity than the other two cases. Hence, it is decided to proceed for further analysis with 2 cm basin water depth.

Effect of square tubular fins on productivity

Figure 7 compares the productivity of conventional and modified solar still at the same basin water depth of 2 cm. The graph indicates that the rate of increase in productivity for both the stills increases gradually with minimum deviation till 12.00 h. As the intensity of solar radiation increases during the post noon session, the deviation in the productivity between the two stills also increases. The
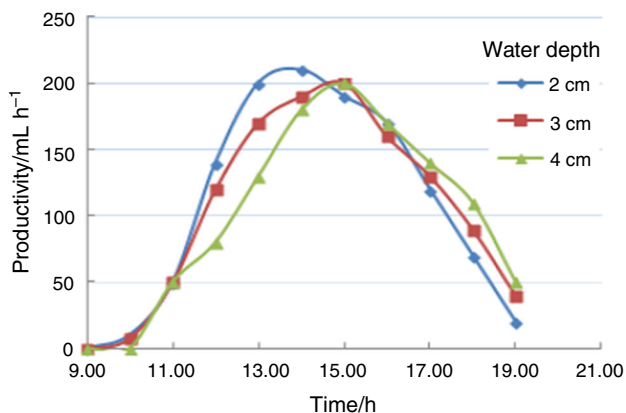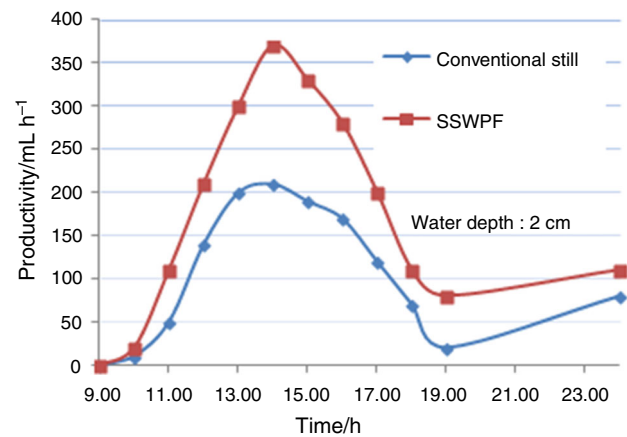
Fig. 7 Comparison of productivity of conventional still and SSWPF

nocturnal productivity of the modified still is found to be 38% more than the conventional still.

Figure 8 gives the comparison between the cumulative distillate outputs of conventional solar still with the modified still. It is observed that the variation in the distillate output between the conventional and modified still begins to increase rapidly after 13:00 h. Also the overnight yield seems to be more for still with fins due to its high energy storage capability, i.e. high heat capacity.

Figure 9 indicates the variation of basin water, glass inner surface and ambient air temperatures with respect to time. It is observed that the basin water temperatures of conventional and modified still raise uniformly till 11.00 h and thereafter the temperature of modified still is found to be more than the conventional still water temperature till the end of the day. The reason for the increase in water temperature of modified still is not only due to increase in heat capacity of the basin by the addition of fins to the basin liner but also due to the reduced mass of the water in the modified still for the same depth.
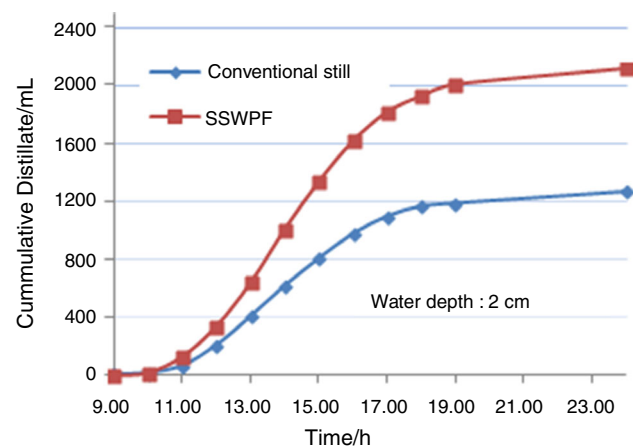
Fig. 6 Hourly variation of productivity with time for different basin water depths

Fig. 8 Comparison of cumulative distillate output of conventional still and SSWPF with respect to time
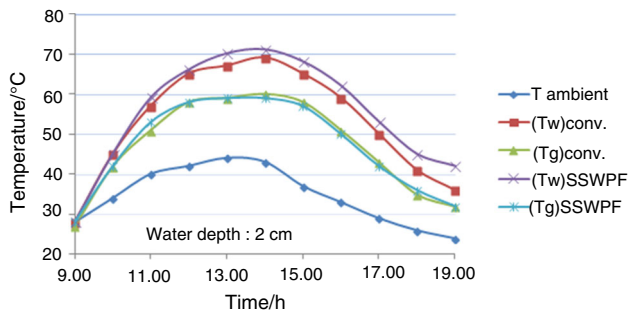
Fig. 9 Hourly variation of temperatures of basin water, glass inner surface and ambient air

Figure 10 illustrates the comparison of hourly variation of temperature difference between the basin water and glass cover inner surface temperature with solar insolation. The temperature of the modified still basin water gets heated up quickly since the area to absorb the incoming solar radiation is increased by attaching fins to the basin liner. This is due to high heat capacity of the modified still basin created by the addition of mass to it in the form of fins though both the basins are made up of same material. In the case of conventional solar still, as it has low heat capacity, the temperature of the water starts to decrease rapidly upon fall in intensity of solar radiation which is evident between 15.00 and 19.00 h.

Figure 11 compares the instantaneous efficiency curve of conventional and modified still. It is inferred that the efficiency of the conventional still is slightly higher than the modified still till noon and during the afternoon session a tremendous change in the scenario has been noticed with peak efficiency for the modified still obtained during 14.00 h. During the dusk, the efficiency of the modified still increases significantly since the addition of fins increased the heat capacity of the basin and hence the
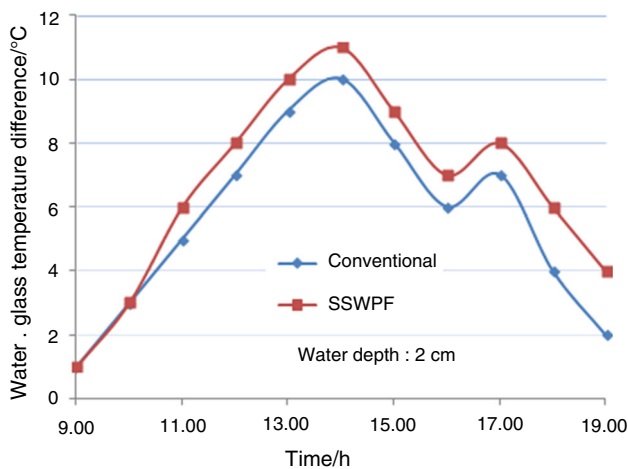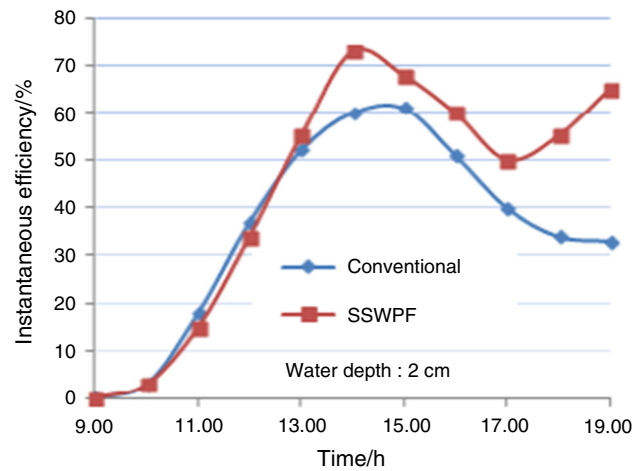

Fig. 11 Comparison of instantaneous efficiency of conventional still and SSWPF

temperature of the water is retained at higher level even during low sunshine hours.

Effect of combined square tubular fin and energy storage on productivity

Figure 12 shows the productivity comparison of conventional still and still with square tubular fins filled with 3 kg of thermal energy storage material. It is observed that the productivity is higher in conventional still till the intensity of the solar radiation is high and experiences a sharp fall when the solar insolation dropped. In contrast, the productivity of the still with square tubular fins and thermal energy storage found to be considerable during declination of solar radiation and even after sunshine hours increasing the overall efficiency of the system. The daily productivity of the modified still has almost doubled when compared
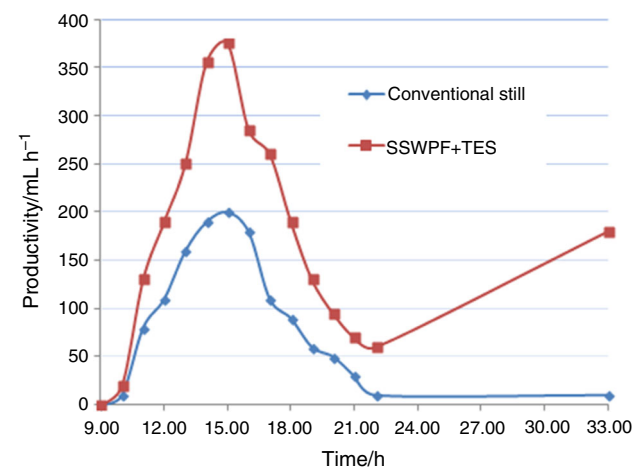

Fig. 10 Hourly variation of temperature difference between basin water and glass inner surface compared with solar radiation

Fig. 12 Comparison of productivity of conventional still and SSWPF + TES

with the conventional still. This result is compared with the outcome of various other researchers as shown in Table 2. It is observed that this research outcome supersedes the previous experimental results [16–22].

Figure 13 illustrates the hourly variation of exergy efficiencies of conventional and modified still. The exergy efficiency of the still remains well below 10% during daytime and gradually starts to increase during off-sunshine hours due to reducing exergy destruction caused by the thermal energy storage material. The reduced exergy destruction in various components of the still increased the exergy efficiency of the still with energy storage during night time. The steep increase in the exergy efficiency after 16.00 h is due to higher heat transfer rate between the basin liner and saline water as well as between water surface and glazing inner surface. This led to reduced exergy destruction in both the cases.

As observed from Fig. 14, the instantaneous efficiency of conventional still has a slight edge over the still with fins and energy storage till noon. During afternoon session, the hourly efficiency of conventional still experiences a steep raise till 14.00 h and started to decline thereafter. But the hourly efficiency of still with fins and energy storage shows a gradual increase till the end of the day due to energy supply from the paraffin wax, which has stored energy during peak sunshine hours. The exergy efficiency of the conventional still is well below 10% throughout the day while the exergy efficiency of still with fins and energy storage has started to increase after 16.00 h and reached its peak value of 74% during night time. The higher exergy efficiencies during off-sunshine hours are also observed by Asbik et al. [28] who have presented the exergy analysis of a passive solar still coupled with heat storage system. It is observed that the instantaneous exergy efficiency of the solar still is less than 5% during the daytime but during night time the exergy efficiency reached above 80% in some cases. During the off-sunshine hours, the latent heat is transferred near isothermally from the PCM to the basin water. This results in reduced irreversibility thereby reducing exergy destruction to a greater extent and hence,
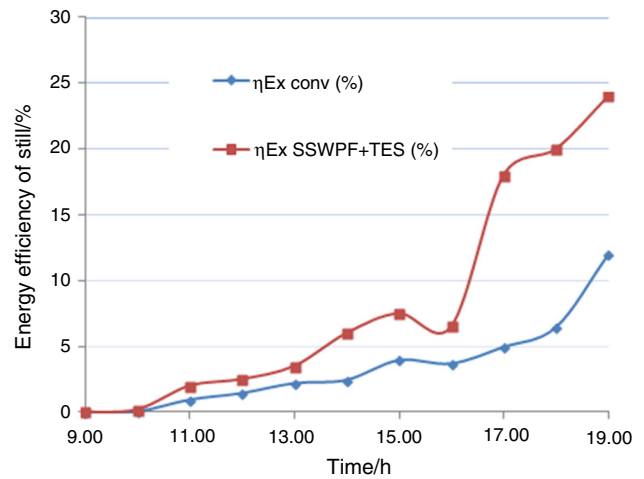

Fig. 13 Comparison of hourly variation of exergy efficiencies of the conventional and SSWPF + TES
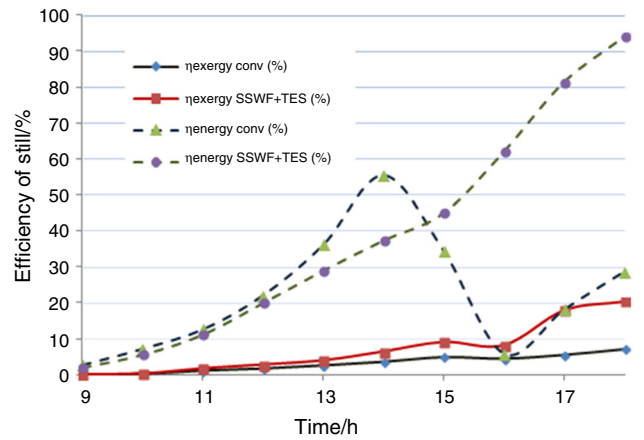

Fig. 14 Comparison of energy and exergy efficiencies of conventional still and SSWPF + TES

the exergy efficiency of the still increased up to 74%. Further, Dincer and Cengel [29] have demonstrated that the exergy efficiency of a solar system would be higher if the heat is retrieved from thermal storage system at higher useful temperatures. As discussed earlier, the modified still

Table 2 Performance comparison of stills for different modifications [20–24]

Sl.no.	Authors	Modifications incorporated	% increase in productivity
1	Omar et al.	Vertical finned still	40
		Corrugated still	21
2	El.Sebaii et al.	Vertical finned still	13.7
3	Alaian et al.	Pin-finned wick surface	23
4	Rajaseenivasan et al.	Square finned still	36.7
		Square fins with wick surface	45.8
5	Velmurugan et al.	Vertical finned still	45.5
6	Present work	Pin-finned still	64
		Pin-finned still with energy storage	95

Table 3 Accuracy, range and percentage error of the measuring instruments

Sl.no	Instrument	Accuracy	Range	Least value measured	Percentage error
1	Thermocouple	$\pm$ 0.1 °C	0–100 °C	28 °C	0.357
2	Temperature Indicator	+ 1 °C	0–300 °C	28 °C	3.57
3	Solarimeter	$\pm$ 1 W m^{-2}	0–2500 W m^{-2}	30 W m^{-2}	3.33
4	Collecting jar	$\pm$ 10 mL	0–1000 mL	100 mL	10

possesses higher temperature than conventional still due to storage system which of course contributes to the higher exergy efficiency.

Error analysis

Error analysis is the study of uncertainties in the physical measurements in the experimentation. The percentage errors associated with measuring instruments thermocouple, temperature indicator, solarimeter and distillate measuring jar were calculated using the following expression suggested in Velmurugan et al. [24];

$$\text{Error} = \frac{\text{Accuracy of the instrument}}{\text{Minimum value of the output measured}} \times 100\%$$

The details of the accuracy, range and percentage error for various measuring instruments used for experimentation are furnished in Table 3.

Conclusions

The performance of a single slope single basin conventional solar still and a similar type of solar still incorporated with square tubular fins attached to the basin liner is investigated. The following conclusions are arrived from the experimental results;

(1) Productivity of both conventional and modified stills increases with decreasing water depth in the basin.

(2) The daily efficiencies of the finned solar still have increased to 68, 58 and 54% when the water depth in the basin is maintained at 2, 3 and 4 cms, respectively.

(3) The daily efficiency of the conventional still, still with fins and still with both fins and energy storage are achieved as 23, 36 and 44%, respectively.

(4) Addition of fins to the basin liner and paraffin wax (energy storage media) increased the nocturnal productivity by 2 times and 5 times, respectively.

(5) The maximum instantaneous energy efficiencies achieved for conventional and still with both fins and energy storage are 55% and 94% during daytime.

(6) The exergy efficiencies achieved for conventional and still with both fins and energy storage are 7% and 20% during daytime. However, the exergy efficiency of the modified still raised up to 74% during night time.

References

1. World Health Organization (WHO) Drinking water facts. 2017. http://www.who.int/mediacentre/factsheets/fs391/en/. Accessed 17 July 2017.
2. Liu L, Johnson HL, Cousens S, Perin J, Scott S, Lawn JE, Rudan I, Campbell H, Cibulskis R, Li M, Mathers C, Black RE. Global, regional, and national causes of child mortality: an updated systematic analysis for 2010 with time trends since 2000. Lancet. 2012;379:2151–61.
3. Chenoweth J. Minimum water requirement for social and economic development. Desalination. 2008;229:245–56.
4. Sathish Kumar TR, Raja Bharathi B. Effect of water depth on productivity of solar still with thermal energy storage. Int J Sci Res. 2013;02:413–7.
5. Gopal C, Mohanraj M, Chandramohan P, Chandrasekar P. Renewable energy source water pumping systems - A literature review. Renew Sustain Energy Rev. 2013;25:351–70.
6. Gopal C, Mohanraj M, Chandramohan P, Sakthivel M, Shepherd B. Modeling of a solar photovoltaic water pumping system under the influence of panel cooling. Therm Sci. 2017;21(2):S399–410.
7. Belyayev Y, Mohanraj M, Jayaraj S, Kaltayev A. Thermal performance simulation of a heat pump assisted solar desalination system for Kazakhstan climatic conditions. Heat Trans Eng. 2018. https://doi.org/10.1080/01457632.2018.
8. Shakir Y, Mohanraj M, Belyayev Y, Jayaraj S, Kaltayev A. Numerical simulation of a heat pump assisted regenerative solar still for cold climates of Kazakhstan. Bulg Chem Commun. 2016;48:126–32.
9. Jegadheeswaran S, Pohekar SD. Performance enhancement in latent heat thermal storage system: a review. Renew Sustain Energy Rev. 2009;13:2225–44.
10. Kumar S, Tiwari G. Life cycle cost analysis of single slope hybrid (PV/T) active solar still. Appl Energy. 2009;86:1995–2004.
11. Kalogirou S. Seawater desalination using renewable energy sources. Prog Energy Combust Sci. 2005;31:242–81.
12. Hay HR. Plastic solar stills: past, present and future. Solar Energy. 1973;14:393–404.
13. Velmurugan V, Gopalakrishnan M, Raghu R, Srithar K. Single basin solar still with fin for enhancing productivity. Desalination. 2008;49:2602–8.
14. Yessen S, Yerzhan B, Mohanraj M, Jayaraj S. Numerical simulation of a heat pump assisted regenerative solar still working

with and without heat storage for cold climate of Kazakhstan. Therm Sci. 2017;21(Supple 2):S411–8.

15. SathishKumar TR, Muthuvasan SR, Kumar D, Kanivel K. Performance analysis on regenerative heat exchanger with paraffin wax as phase change material. Int J Appl Eng Res. 2015;10(85):599–603.

16. SathishKumar TR, BharaniShankar G, GaneshBalaji S. Review on solar still with thermal energy storage. Int J Appl Eng Res. 2015;10(85):621–7.

17. Ramadan MRI. Effect of fin configuration parameters on single basin solar still performance. Desalination. 2015;365:15–24.

18. Rabhi K, Nciri R, Nasri F, Ali C, Bacha HB. Experimental performance analysis of a modified single-basin single-slope solar still with pin fins absorber and condenser. Desalination. 2017;416:86–93.

19. Panomwan R, Ayuthaya N, Namprakai P, Ampun W. The thermal performance of an ethanol solar still with fin plate to increase productivity. Renew Energy. 2013;54:227–34.

20. Omar ZM, Hamid MH, Kabeel AE. Performance of finned and corrugated absorbers solar stills under Egyptian conditions. Desalination. 2011;277:281–7.

21. El-Sebaii AA, Ramadan MRI, Aboul-Enein S, El-Naggar M. Effect of fin configuration parameters on single basin solar still performance. Desalination. 2015;365:15–24.

22. Alaian WM, Elnegiry EA, Hamed AM. Experimental investigation on the performance of solar still augmented with pin-finned wick. Desalination. 2016;379:10–5.

23. Rajaseenivasan T, Srithar K. Performance investigation on solar still with circular and square fins in basin with CO_2 mitigation and economic analysis. Desalination. 2016;380:66–74.

24. Velmurugan V, Deenadayalan CK, Vinod H, Srithar K. Desalination of effluent using fin type solar still. J Energy. 2008;33:1719027.

25. Srivastava PK, Agrawal SK. Winter and summer performance of single sloped basin type solar still integrated with extended porous fins. Desalination. 2013;319:73–8.

26. El-Sebaii AA, El-Naggar M. Year round performance and cost analysis of a finned single basin solar still. Appl Therm Eng. 2017;110:787–94.

27. Sharshir SW, Elsheikh AH, Peng G, Yang N, El-Samadony MOA, Kabeel AE. Thermal performance and exergy analysis of solar stills—a review. Renew Sustain Energy Rev. 2017;73:521–44.

28. Asbik M, Ansari O, Bah A, Zari N, Mimet A, El-Ghetany H. Exergy analysis of solar desalination still combined with heat storage system using phase change material (PCM). Desalination. 2016;381:26–37.

29. Dincer I, Cengel YA. Energy, entropy and their roles in thermal engineering. Entropy. 2001;3:116–49.